

FM-CW LiDAR for Proximity Sensing Applications Integrating an Alignment-Tolerant FSO Data Channel

Aina Val Marti, Thomas Zemen, and Bernhard Schrenk

AIT Austrian Institute of Technology, 1210 Vienna, Austria. aina.val-marti@ait.ac.at

Abstract We experimentally demonstrate the integration of a 1.25 Gb/s FSO data channel in a FM-CW LiDAR and evaluate the sensing vs. comms performance trade-off when making the data channel robust to receiver misalignment through an expanded, fan-shaped LiDAR beam. ©2022 The Author(s)

Introduction

Light detecting and ranging (LiDAR) technology has been of great interest in many applications such as autonomous driving, remote sensing or 3D imaging. LiDAR builds on a time-of-flight (ToF) measurement [1, 2] over a high optical path loss budget, as it is supported through pulsed high-power VCSELs in combination with single-photon APDs [3] or through coherent detection of frequency-modulated continuous-wave (FMCW) light [4]. The latter offers high resolution by exploiting the large frequency bandwidth available in the optical domain [5, 6], as evidenced through the demonstration of an accuracy in the range of 150 μm in [7].

One attractive aspect for many LiDAR applications is the possibility to combine the ranging of targets with free-space optical (FSO) communications. For example, platooning requires a precise tracking of adjacent vehicles and their surroundings, while communication allows to see through these neighbouring cars by sharing information on the overall situational awareness within the platoon. The technology overlap between sensing and communication systems permits a multi-purpose use of optoelectronic hardware. FM-CW LiDAR squarely fits to this context [5, 8] as it derives from the field of coherent optical telecommunications.

In this work, we investigate the functional integration of an alignment-tolerant FSO communication channel in a fixed- λ FM-CW LiDAR. We experimentally evaluate the dual-purpose sensing/comms transceiver for close-proximity applications and prove the robustness and trade-offs for simultaneous FSO communication to lateral receiver misalignment.

FM-CW LiDAR with Integrated FSO Comms

FM-CW LiDAR differs from other LiDARs in how information about the distance is retrieved by involving a frequency-modulated optical carrier. Whereas a ToF system directly measures the travelled time to an object, the FM-CW concepts mixes the returning signal with a reference to indirectly measure the time: First, a continuous-

wave laser is linearly frequency modulated over a span ΔF within a period T (with rate $R = \Delta F/T$), providing a triangular frequency sweep (Fig. 1).

This frequency sweep can be achieved through modulation of the driving current of a diode laser, or through an external modulator using a more sophisticated laser [9, 10]. In this work we build on an RF-based FM method in combination with a single-wavelength laser. We thus avoid complex calibration due to laser non-linearity and further retain a degree of freedom for the optical emission frequency that could be later exploited to accomplish the steering of the (fan-shaped) light beam in a second dimension. An I/Q modulator accomplishes the required carrier-suppressed single-sideband (CS-SSB) modulation. The swept light is then used for probing and as local oscillator (LO) for the detection of back-scattered light, which provides information on an object in the field-of-view as it is now frequency-shifted according to (i) the Doppler shift and (ii) the ToF delay. These can be extracted from the average and difference frequencies of the induced beat terms [1, 4].

A communication channel is embedded through intensity modulation before the light is transmitted. The corresponding optical field can be expressed as

$$E = \cos\left(\frac{\pi\mu}{2V_\pi}\delta(t) + \frac{\pi}{4}\right) \exp\left(2\pi jt\left(v + f_c + \frac{\Delta F}{2} + \left(1 - \Delta F\left|\frac{2t}{T} - 1\right|\right)\right)\right)$$

where $\delta(t)$ is the baseband data signal, V_π is the half-wave voltage of the Mach-Zehnder modulator (MZM) employed for intensity modulation, μ is the modulation index, v is the optical emission frequency and f_c an offset for the triangular frequency modulation.

Phase-diversity coherent reception permits a

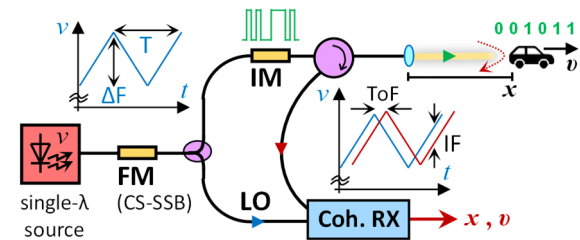


Fig. 1: FSO communication on FMCW probe light.

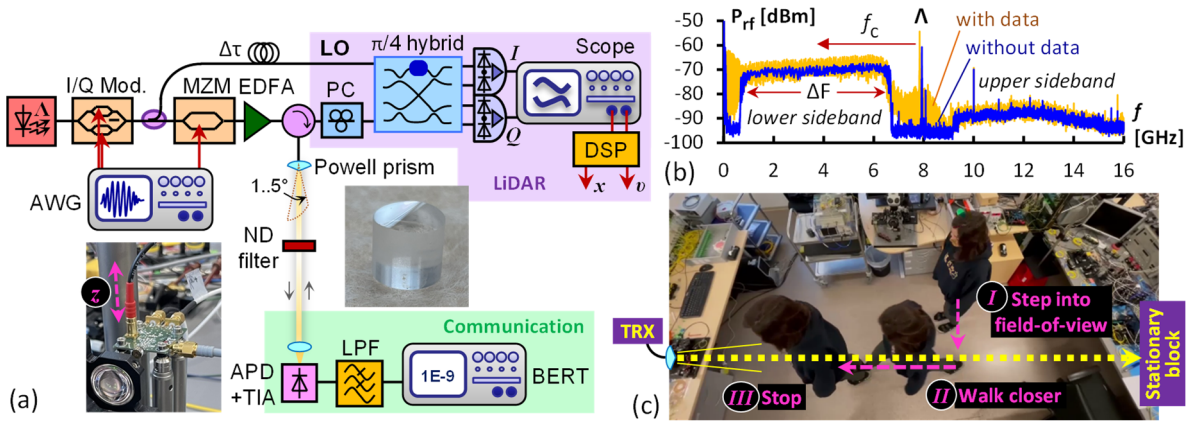


Fig. 2: (a) Experimental setup. (b) Spectrum of the OCS-SSB FM light. (c) Scenario for evaluating the LiDAR function.

retrieval of the distance and the velocity of the object reflecting the probe light through extracting the Doppler shift that is superimposed on the beat note resulting from the optical echo and the LO [4]. The data stream embedded with the probe light can be retrieved with a simple, frequency-agnostic direct-detection receiver.

Experimental Setup

The experimental setup is shown in Fig. 2a. A laser with a wavelength of $\Lambda = 1550.50$ nm and a linewidth of 1.4 kHz is optically frequency-swept by an I/Q modulator by means of CS-SSB modulation. The triangular sweep function had a period of 890 μ s and the optical frequency deviation was $\Delta F = 6$ GHz and centred at $f_c = 4.25$ GHz relative to the optical carrier (Λ). This allows for a resolution of less than 5 cm. The frequency modulated light, whose heterodyned spectrum is reported in Fig. 2b, is then split to probe the scene and to serve as the LO for the phase-diversity coherent receiver. The portion of the signal used for sensing is further encoded with $R_b = 1.25$ Gb/s PRBS on-off keyed data at a modulation index of $\mu = 0.5$ using a MZM. The signal is then amplified by an EDFA and launched to the remote object using either a collimation lens as reference, or 9-mm Powell prisms with fan angle of 1° or 5° to accomplish alignment-tolerant FSO reception.

We chose a person walking a predefined path as the moving object under test (Fig. 2c). The reflection is collected by the lens/prism and a circulator is used as directional split towards the optical 90° hybrid before balanced homodyne detection. A short delay fiber ($\Delta\tau$) in the LO path minimizes the intermediate frequency (IF) for coherent detection by accounting for the optical path delay caused by the EDFA and other fiber-optic components. The I and Q components of the detected light are acquired by a real-time oscilloscope.

Offline digital signal processing finally yields the distance x and velocity v of the moving

object. The communication function has been evaluated through BER measurement. For this, the object is replaced by a direct-detection receiver comprising of a 1-inch collimation lens and a TO-can APD receiver. A 1-GHz lowpass filter rejects the residual out-of-band signature deriving from the optical frequency sweep.

It shall be stressed that all FM-CW transceiver elements can be readily realized on PIC platforms, given the possible replacement of EDFA and circulator through SOA and highly directional 50/50 coupler, respectively.

Results and Discussion: LiDAR Sensing

Figure 3a shows an acquired spectrogram using the collimated lens. The constant beat terms ρ in the range from 500 to 650 kHz derive from an optical echo in the bidirectional fiber path, such as it results due to the finite directivity of the circulator, the weak Fresnel reflection at the FC/APC connector, and the distributed Rayleigh backscattering of its fiber pigtail. The beat notes further indicate the IF set through $\Delta\tau$ to minimize the required sampling rate for data acquisition. The spectrogram shows the superimposed beat notes due to the object in the free-space path: Before moment I , a stationary blocking object is ranged. At I , a person steps into the field of view and then walks towards the LiDAR transceiver (II). Finally, the motion of the object stops (III).

Figure 3b and 3c present the extracted information on position x and velocity v . Results are shown for collimated (\diamond) and fan-shaped (\circ, \bullet, \times) LiDAR beams using the same walk pattern, while further making comparison between a present and an absent FSO data channel. We did not observe a loss of sensitivity for present FSO data with the collimated beam, which can resolve position and velocity accurately over the entire range (\diamond). A similar performance applies for the 1° Powell prism (\circ), whereas additional FSO data leads to a reduced accuracy for distances of >3 m due to beat noise (\bullet). The same limitation applies to a 5°

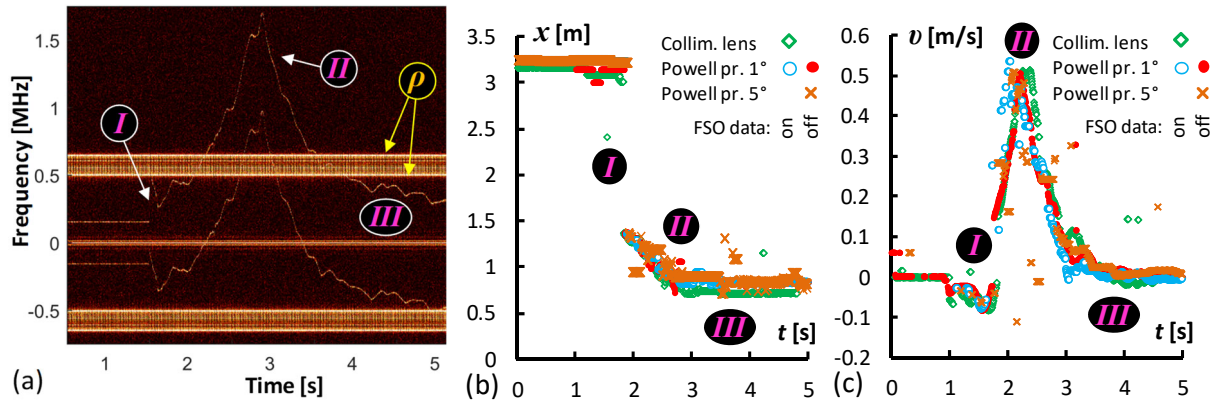


Fig. 3: (a) Spectrogram for LiDAR sensing and extracted information on (b) the distance and (c) velocity of a moving object.

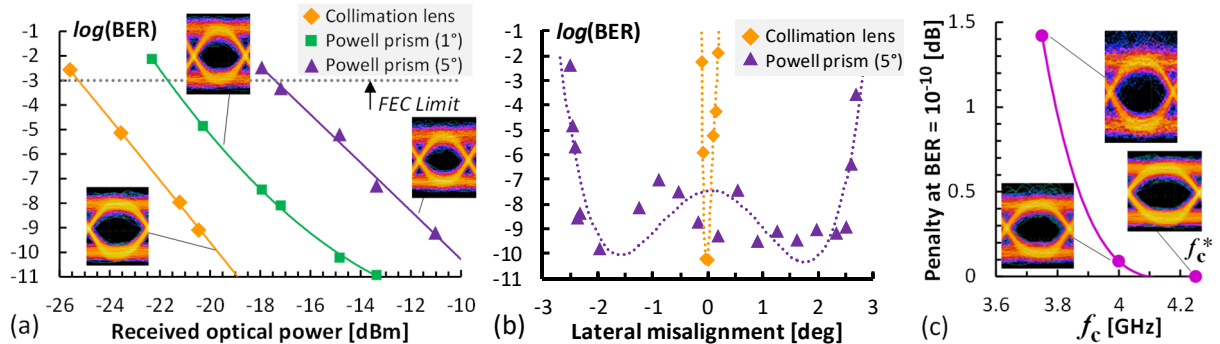


Fig. 4: (a) BER performance for FSO communication and (b) its alignment tolerance. (c) Dependence on sweep parameter f_c .

fan-shaped beam (\times), even without FSO data, for which the distance information resembles that of the other scenarios, while information on the velocity shows large errors. This is attributed to the fading received optical power coupled back to the fiber for a wider fan angle. It could be partially compensated by a more powerful LO, which, given the RF-based FM sweep, experiences a high CS-SSB modulation loss.

Integrated FSO Communication Channel

The BER performance over the FSO path has been evaluated as function of the received optical power. For this purpose, neutral-density (ND) filters are inserted between the LiDAR emission port and the APD receiver. Figure 4a reports the BER for using a collimation lens (\blacklozenge) and the Powell prism with 1° (\blacksquare) and 5° (\blacktriangle) fan angle. We noticed a 4.7 dB penalty at a BER of 10^{-10} between the collimated and the narrower fan beam. This is attributed to the spatial distribution of the launched fan-shaped LiDAR beam over its proximity propagation distance of 3.2 m. However, the reception becomes tolerant to the alignment. To prove this point, we have laterally misplaced the APD receiver from the optical axis of the LiDAR system (z in Fig. 2a). As Fig. 4b shows, the expanded field of illumination can account for an angular range of 5.4° within which communication can be established. This range corresponds to the 5° fan angle of the Powell prism and stands in

strong contrast to the collimated beam, which requires a very precise alignment ($\pm 0.14^\circ$).

Finally, we have characterized the reception penalty when lowering the sweep parameter f_c , which would eventually cause the residual optical carrier (Δ in Fig. 2b) to beat with the data signal. We took the original setting of $f_c^* = 4.25$ GHz (corresponding to the BER of Fig. 4a) as a reference since the carrier is then spaced by the symbol rate R_b towards the data signal. When lowering f_c , which would be seen as beneficial for a higher R_b due to the more relaxed RF drive frequencies, the penalty rises and already reaches a 1-dB value at 3.95 GHz or $0.93 f_c^*$.

Conclusions

We have experimentally evaluated a FM-CW LiDAR transceiver for FSO communications at 2.5 Gb/s in a proximity scenario. Simultaneous sensing and data transmission operation was found feasible despite fan-shaped LiDAR beams. The requirements concerning receiver alignment for FSO data transmission can be greatly relaxed according to an expanded fan-shaped beam, though requiring a trade-off with the accomplishable sensitivity for sensing. The RF-based FM sweep, which is supported by the telecom-centric broadband opto-electronics employed for the LiDAR hardware, would further permits the steering of the fan-shaped LiDAR beam in the second dimension by means of wavelength tuning, which is left for future work.

Acknowledgements

This work was supported by the ERC under the EU Horizon-2020 programme (grant n° 804769) and by the Austrian FFG agency through the LIANDRI project (grant n° 861571).

References

- [1] S. Royo and M. Ballesta-Garcia, "An overview of lidar imaging systems for autonomous vehicles," *Applied Sciences*, vol. 9, no. 19, p. 4093, 2019. DOI: 10.3390/app9194093.
- [2] B. Behroozpour, P. Sandborn, M.C. Wu, and B.E. Boser, "Lidar System Architectures and Circuits," *IEEE Communications Magazine*, vol. 55, no. 10, pp. 135-142, 2017. DOI: 10.1109/MCOM.2017.1700030.
- [3] S. Jahromi, J.P. Jansson, and J. Kostamovaara, "Solid-state 3D imaging using a 1nJ/100ps laser diode transmitter and a single photon receiver matrix," *Optics Express*, vol. 24, no. 19, pp. 21619-21633, 2016. DOI: 10.1364/OE.24.021619.
- [4] P. Feneyrou, L. Leviandier, J. Minet, G. Pillet, A. Martin, D. Dolfi, J.-P. Schlotterbeck, P. Rondeau, X. Lacondemine, A. Rieu, and T. Midavaine, "Frequency-modulated multifunction lidar for anemometry, range finding, and velocimetry-1. Theory and signal processing," *Applied Optics*, vol. 56, no. 35, pp. 9663-9675, 2017. DOI: 10.1364/AO.56.009663.
- [5] Z. Xu, K. Chen, X. Sun, K. Zhang, Y. Wang, J. Deng, and S. Pan, "Frequency-Modulated Continuous-Wave Coherent Lidar With Downlink Communications Capability," *Photonics Technology Letters*, vol. 32, no. 11, pp. 655-658, 2020, DOI: 10.1109/LPT.2020.2990942.
- [6] A. Martin, D. Dodane, L. Leviandier, D. Dolfi, A. Naughton, P. O'Brien, T. Spuessens, R. Baets, G. Lepage, P. Verheyen, P. De Heyn, P. Absil, P. Feneyrou, and J. Bourderionnet, "Photonic integrated circuit-based FMCW coherent LiDAR," *Journal of Lightwave Technology*, vol. 36, no. 19, pp. 4640-4645, 2018. DOI: 10.1109/JLT.2018.2840223.
- [7] E. Baumann, J.D. Deschenes, F.R. Giorgetta, W.C. Swann, I. Coddington, and N.R. Newbury, "Speckle phase noise in coherent laser ranging: fundamental precision limitations," *Optics Letters*, vol. 39, no. 16, pp. 4776-4779, 2014. DOI: 10.1364/OL.39.004776.
- [8] Z. Li, Z. Zang, M. Li, and H.Y. Fu, "LiDAR integrated high-capacity indoor OWC system with user localization capability," in *Proc. Optical Fiber Communication Conference (OFC)*, 2021, paper Tu5E.2. DOI: 10.1364/OFC.2021.Tu5E.2.
- [9] S. Gao and R. Hui, "Frequency-modulated continuous-wave lidar using I/Q modulator for simplified heterodyne detection," *Optics Letters*, vol. 37, no. 11, pp. 2022-2024, 2012. DOI: 10.1364/OL.37.002022.
- [10] G. Pillet, L. Morvan, M. Brunel, F. Bretenaker, D. Dolfi, M. Vallet, J.-P. Huignard, and A. Le Floch, "Dual-frequency laser at 1.5 μm for optical distribution and generation of high-purity microwave signals," *Journal of Lightwave Technology*, vol. 26, no. 15, pp. 2764-2773, 2008. DOI: 10.1109/JLT.2008.927209.